# Power Spectral Density Limitations of the Wavelet-OFDM System

Marwa Chafii *, Jacques Palicot *, Rémi Gribonval † and Alister G. Burr ‡
* CentraleSupélec, IETR, Campus de Rennes
35576 Cesson - Sévigné Cedex, France
Email: {marwa.chafii, jacques.palicot} @supelec.fr
†Inria - Bretagne Atlantique, 35042 Rennes Cedex, France
Email: remi.gribonval@inria.fr
‡Dept. of Electronics University of York, York, UK
Email: alister.burr@york.ac.uk

***Abstract*—Wavelet-OFDM based on the discrete wavelet transform is a multicarrier modulation technique of considerable interest, due to its good performance in several respects such as the peak-to-average power ratio and the interference cancellation, as investigated in the literature. More specifically, the Haar wavelet has been proposed by various researchers as the most attractive wavelet for data transmission. In this paper, we address the power spectral density limitations of Wavelet-OFDM, and we show analytically and experimentally that the bandwidth efficiency of Haar Wavelet-OFDM is significantly poorer than OFDM, having larger main lobe and side lobes compared with OFDM, which reduces the attractiveness of the scheme.**

***Keywords*—*Wavelet-OFDM, Orthogonal Frequency Division Multiplexing (OFDM), Haar wavelet, Discrete Wavelet Transform (DWT), Power Spectral Density (PSD).***

## I. Introduction

Orthogonal frequency division multiplexing (OFDM) is a very popular modulation technique used in many wireless and wireline communication standards, thanks to its high spectral efficiency and its ability to overcome the effects of multipath channels. However, OFDM suffers from some drawbacks such as high peak-to-average power ratio (PAPR), and sensitivity to carrier frequency offset and synchronisation errors. To counter these disadvantages, much research has been conducted in order to design new multi-carrier modulation (MCM) systems as alternatives to OFDM. In this context, Wavelet-OFDM [1], also known as orthogonal wavelet division multiplexing (OWDM) [2], has been proposed and promoted by many authors. Wavelet-OFDM modulation is based on the inverse discrete wavelet transform (IDWT) instead of the inverse discrete Fourier transform (IDFT) as for OFDM. In [3], the authors claim that the Haar and the Daubechies wavelets outperform conventional OFDM in reducing inter-symbol interference and inter-carrier interference in the power line communication context. According to [4] and [5], the Haar wavelet outperforms OFDM and the other wavelets in terms of bit error rate. The Haar wavelet has been also presented as the wavelet that gives the best PAPR performance [6], [5] and the lowest computation complexity [7].

However, the bandwidth efficiency of Wavelet-OFDM has been rarely addressed in the literature. The common belief is that Wavelet-OFDM improves the bandwidth efficiency compared with OFDM, since it does not need a cyclic prefix as stated in many references [5], [7], [8], [9], [10]. However, there are other factors which may have a more significant effect on bandwidth efficiency, and this has motivated us to conduct a more rigorous study of the power spectral density (PSD) of Wavelet-OFDM, which highlights, as we will see, the cost to pay for the advantages enumerated above, especially in the case of the Haar wavelet.

In this paper, we study analytically and experimentally the PSD of Wavelet-ODFM, and specifically for the Haar wavelet, since this latter has been promoted in the literature for its several advantages, but its limitations have rarely been investigated. We show that the bandwidth efficiency of Haar Wavelet-OFDM is poorer than conventional OFDM, having large main lobe and side lobes compared with OFDM. We also addressed the PSD problem as a serious limitation of the Wavelet-OFDM, which should be taken carefully in the study of this new modulation technique.

The paper is organized as follows. Section II defines the Wavelet-OFDM and its variants. The theoretical analysis of the PSD is presented in Section III, while Section IV presents the simulation of the PSD that confirms our analytical result, and further discussions. The conclusions are drawn in Section V with some perspectives of the work.

## II. Description of the Wavelet-OFDM system

*Notations:* The transmitted MCM signal can be expressed in general as:

$$x(t) \quad = \quad \sum_{n\in\mathbb{Z}} \sum_{m=0}^{M-1} C_{m,n} \underbrace{g_m(t-nT_0)}_{g_{m,n}(t)}. \qquad (1)$$

$M$ denotes the number of carriers. $C_{m,n}$ stands for the input complex symbol, time index $n$, modulated by carrier index $m$. Let us assume that $(C_{m,n})_{(m\in[\![0,M-1]\!],\, n\in\mathbb{Z})}$ are independent and identically distributed, with zero mean and unit variance $\sigma_C^2$. $T_0$ is the duration of $M$ input symbols $C_{m,n}$ (duration of the MCM symbol). The modulation transform and the pulse shaping filter are jointly modeled by a single function denoted by $g_m \in L^2(\mathbb{R})$ (the space of square integrable functions).

978-0-9928-6265-7/16/$31.00 ©2016 IEEE

### A. Expression of the transmitted signal

Wavelet-OFDM is an MCM system based on the Wavelet basis instead of the Fourier basis. The modulation system $(g_m)_{m\in[\![0,M-1]\!]}$ is represented by the wavelet functions $(\psi_{j,k})_{j\in[\![J_0,J-1]\!],k\in[\![0,2^j-1]\!]}$ and the scaling functions $(\phi_{J_0,k})_{k\in[\![0,2^{J_0}-1]\!]}$ of the first scale. The waveforms $(g_m)_{m\in[\![0,M-1]\!]}$ can be expressed as:

$$(g_m)_{m\in[\![0,M-1]\!]} := \begin{cases} (\psi_{J_0,k})_{k\in[\![0,2^{J_0}-1]\!]} \cup (\phi_{J_0,k})_{k\in[\![0,2^{J_0}-1]\!]}, \\ \quad \text{if} \quad m \in [\![0, 2^{J_0+1}-1]\!] \\ (\psi_{j,k})_{j\in[\![J_0,J-1]\!],k\in[\![0,2^j-1]\!]} \\ \quad \text{else.} \end{cases}$$

The transmitted Wavelet-OFDM signal is then defined as follows:

$$\begin{aligned} x(t) &= \sum_n \sum_{j=J_0}^{J-1} \sum_{k=0}^{2^j-1} w_{j,k}\psi_{j,k}(t-nT_0) \\ &\quad + \sum_n \sum_{q=0}^{2^{J_0}-1} a_{J_0,q}\phi_{J_0,q}(t-nT_0). \end{aligned} \quad (2)$$

- $J-1$: last scale considered, with $M = 2^J$,
- $J_0$: first scale considered ($J_0 \leq j \leq J-1$),
- $w_{j,k}$: wavelet coefficients located at $k$-th position from the scale $j$,
- $a_{J_0,k}$: approximation coefficients located at $k$-th position from the first scale $J_0$,
- $\psi_{j,k} = 2^{j/2}\psi(2^j t - kT_0)$: the wavelet orthogonal functions,
- $\phi_{J_0,k} = 2^{\frac{J_0}{2}}\phi(2^{J_0}t - kT_0)$: the scaling orthogonal functions at the scale $J_0$.

Note that the wavelet coefficients $w_{j,k}$ and the approximation coefficients $a_{J_0,k}$ represent the complex input symbols $C_{m,n}$ of (1). The mother wavelet function and the mother scaling function have a duration of $T_0$, and corresponds to $j = 0, k = 0$. For each scale $j$ corresponds $2^j$ translated wavelet functions. From one scale to the next, the number of wavelet functions is then multiplied by two.

### B. Variants and implementation

Several variants of the Wavelet-OFDM system can be considered, depending on the first scale $J_0$ selected. Since the scaling functions are considered only for the first scale, $J_0$ then defines the number of the scaling functions $\phi_{j,k}$ in the modulation system. Fig.1 depicts the wavelet modulation system for different values of $J_0$, for $M = 8$ carriers. By convention, when $J_0 = J$, there are $2^J$ scaling functions $\phi_{j,k}$ and no wavelet function $\psi_{j,k}$ considered in the wavelet basis. Note that the position of the functions in Fig.1 is not a coincidence, but it has an importance since it gives an idea about the time frequency localization $(\Delta t, \Delta f)$ of the waveforms, which is studied in Section II-C .

In order to implement the Wavelet-OFDM system expressed in (2), we apply the Mallat algorithm [11]. For a Wavelet-OFDM signal based on the wavelets of $L = J - J_0$ scales and the scaling functions of the scale $J_0$, the IDWT should be performed $L$ times. $L$ can be also be interpreted as the number of decomposition levels. Let $\boldsymbol{C_n}$ be a vector of $M$ input complex symbols $C_{m,n}$. The $2^{J_0}$ first $C_{m,n}$ symbols correspond to the $2^{J_0}$ scaling coefficients $(a_{J_0,q})_{q\in[\![0,2^{J_0}-1]\!]}$.

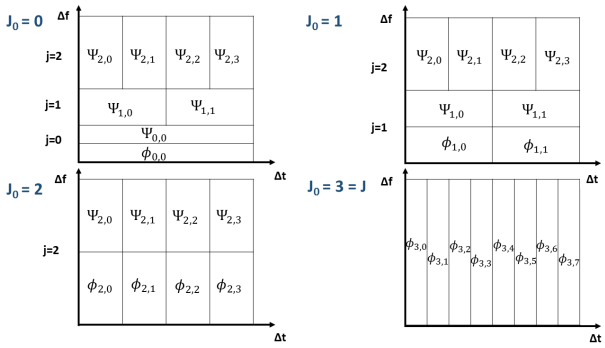


Figure 1: Some variants of the Wavelet-OFDM.

The second $2^{J_0}$ complex symbols corresponds to the wavelet coefficients $(w_{J_0,k})_{k\in[\![0,2^{J_0}-1]\!]}$ of the first scale $J_0$. First, one IDWT is performed, which gives in its output $2^{J_0+1}$ scaling coefficients. After that, the next $2^{J_0+1}$ coefficients from the vector $\boldsymbol{C_n}$ are extracted and considered as wavelet coefficients, and the second IDWT is performed. The next symbols are processed in the same way until the last scale $j = J-1$ is reached. The vector $\boldsymbol{C_n}$ can be expressed then as:

$$\begin{aligned} \boldsymbol{C_n} &= (a_{J_0,0}, a_{J_0,1}, \ldots, a_{J_0,2^{J_0}-1}) \\ &\quad \bullet (w_{J_0,0}, w_{J_0,1}, \ldots, w_{J_0,2^{J_0}-1}) \\ &\quad \bullet (w_{J_0+1,0}, w_{J_0+1,1}, \ldots, w_{J_0+1,2^{J_0+1}-1}) \\ &\quad \bullet \ldots \bullet (w_{j,0}, w_{j,1}, \ldots, w_{j,2^j-1}) \\ &\quad \bullet \ldots \bullet (w_{J-1,0}, w_{J-1,1}, \ldots, w_{J-1,2^{J-1}-1}). \end{aligned} \quad (3)$$

The symbol $\bullet$ in (3) stands for the concatenation operator. Fig.2 defines the implementation of one decomposition level $j$. According to the Mallat algorithm, the IDWT consists of upsampling by a factor of two and filtering the approximation coefficients (scaling coefficients) and the detail coefficients (wavelet coefficients) respectively by a low-pass $f^l$ and a high-pass $f^h$ filter, whose responses are derived from the wavelet considered.

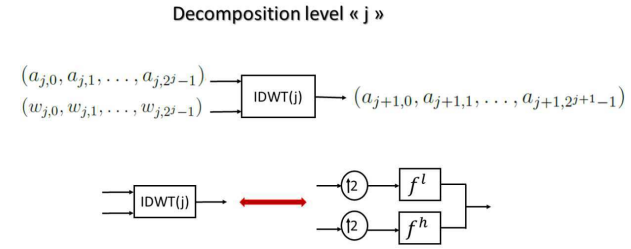


Figure 2: IDWT implementation

### C. Time-Frequency analysis

To characterize the waveform $g_m$ in the time and frequency domain, we usually refer to the first and second moments in these two dimensions, also known as time mean $t_{g_m}$ and frequency mean $f_{G_m}$ for the first order, and time localization (TL) and frequency localization (FL) for the second order.

They are defined as:

$$t_{g_m} = \frac{1}{E_{g_m}} \int_{-\infty}^{+\infty} t|g_m(t)|^2\, dt, \quad (4)$$

$$f_{G_m} = \frac{1}{E_{g_m}} \int_{-\infty}^{+\infty} f|G_m(f)|^2\, df, \quad (5)$$

$$\Delta t_{g_m} = \left(\frac{4\pi}{E_{g_m}} \int_{-\infty}^{+\infty} (t - t_{g_m})^2 |g_m(t)|^2\, dt\right)^{1/2}, \quad (6)$$

$$\Delta f_{G_m} = \left(\frac{4\pi}{E_{g_m}} \int_{-\infty}^{+\infty} (f - f_{g_m})^2 |G_m(f)|^2\, df\right)^{1/2}, \quad (7)$$

$$\text{such that} \quad E_{g_m} = \int_{-\infty}^{+\infty} |g_m(t)|^2\, dt. \quad (8)$$

$E_{g_m}$ is the normalized energy of the waveform $g_m$, assumed to be equal to 1 for all the waveforms $g_m$. $t_{g_m}$ and $f_{G_m}$ can be interpreted as the centre of gravity of the waveform $g_m$ in the time domain and frequency domain respectively, or the averaged normalized time (frequency resp.) centre. We can also say that the spectrum $G_m$ is localized around the frequency $f_{G_m}$. $\Delta t_{g_m}$ and $\Delta f_{G_m}$ can be understood as the duration and the bandwidth of the waveform $g_m$ respectively.

Without loss of generality, let $t_\psi = 0$. The first and second moment of the wavelet functions $(\psi_{j,k})_{j\in[\![J_0,J-1]\!],k\in[\![0,2^j-1]\!]}$ for the time and frequency domain, are deduced from the first and second moment of the mother wavelet function $\psi$ as follows:

$$t_{\psi_{j,k}} = 2^{-j}(t_\psi + kT_0) = 2^{-j}(kT_0), \quad (9)$$

$$f_{\Psi_j} = 2^j f_\Psi, \quad (10)$$

$$\Delta t_{\psi_{j,k}} = 2^{-j}\Delta t_\psi, \quad (11)$$

$$\Delta f_{\Psi_j} = 2^j \Delta f_\Psi. \quad (12)$$

We can observe that, in the time domain, the wavelets of each scale are translated in time, and have the same TL. In the frequency domain, the wavelets of each scale have the same FL, and then occupy the same bandwidth. From one scale to the next, the TL is divided by a factor of 2, and the FL is multiplied by a factor of 2.
The scaling functions $(\phi_{J_0,k})_{k\in[\![0,2^{J_0}-1]\!]}$ verify the same relationship with the scaling mother function.

## III. PSD Analysis

### A. Theoretical analysis of the PSD of Wavelet-OFDM

The Fourier transform of the MCM signal $x(t)$ in (1) is expressed as follows:

$$X(\omega) = \sum_n \sum_{m=0}^{M-1} C_{m,n} G_m(\omega) e^{-i\omega n T_0}. \quad (13)$$

$G_m(\omega)$ is the Fourier transform of $g_m(t)$, and $\omega = 2\pi f$.

**Definition 1.** Auto-correlation function

$$\Gamma_x(t,\tau) := \mathcal{E}(x(t)\bar{x}(t-\tau)), \quad (14)$$

where $\bar{x}$ is the conjugate of $x$, and $\mathcal{E}(.)$ is the expectation operator.

$$\Gamma_x(t,\tau) = \sum_{n,n'} \sum_{m,m'} \mathcal{E}(C_{m,n}\bar{C}_{m',n'}) g_{m,n}(t)\bar{g}_{m',n'}(t-\tau)$$

$$\Gamma_x(t,\tau) = \sum_n \sum_{m=0}^{M-1} g_m(t - nT_0)\bar{g}_m(t - nT_0 - \tau). \quad (15)$$

**Definition 2.** Auto-correlation mean function

$$\bar{\Gamma}_x(\tau) := \frac{1}{T_0}\int_0^{T_0} \Gamma_x(t,\tau)\, dt. \quad (16)$$

Let $\tilde{g}_m(t) = \bar{g}_m(-t)$

$$\begin{aligned}\bar{\Gamma}_x(\tau) &= \frac{1}{T_0}\sum_{m=0}^{M-1}\sum_n \int_0^{T_0} g_m(t - nT_0)\bar{g}_m(t - nT_0 - \tau) \\ &= \frac{1}{T_0}\sum_{m=0}^{M-1}\sum_n \int_{-nT_0}^{-(n-1)T_0} g_m(t)\bar{g}_m(t-\tau) \\ &= \frac{1}{T_0}\sum_{m=0}^{M-1}\int_{-\infty}^{+\infty} g_m(t)\bar{g}_m(t-\tau) \\ &= \frac{1}{T_0}\sum_{m=0}^{M-1}(g_m * \tilde{g}_m)(\tau). \end{aligned} \quad (17)$$

**Definition 3.** Power Spectral Density
*The PSD of a cyclostationary process $x$ is defined as*

$$\gamma_x(\omega) = FT(\bar{\Gamma}_x(\tau)), \quad (18)$$

where FT means the Fourier transform.

$$\begin{aligned}\gamma_x(\omega) &= FT(\frac{1}{T_0}\sum_{m=0}^{M-1}(g_m * \tilde{g}_m)(\tau)) \\ &= \frac{1}{T_0}\sum_{m=0}^{M-1} G_m(\omega)\bar{G}_m(\omega) \\ &= \frac{1}{T_0}\sum_{m=0}^{M-1}|G_m(\omega)|^2. \end{aligned} \quad (19)$$

In the case of the Wavelet-OFDM system, let $\Psi(\omega)$ and $\Phi(\omega)$ be the Fourier transform of $\psi(t)$ and $\phi(t)$ respectively. From (2) and (19), we have:

$$\gamma_{x_{\text{wavelet}}}(\omega) = \frac{1}{T_0}\sum_{j=J_0}^{J-1}\sum_{k=0}^{2^j-1}|\Psi_{j,k}(\omega)|^2 + \frac{1}{T_0}\sum_{q=0}^{2^{J_0}-1}|\Phi_{J_0,q}(\omega)|^2.$$

$$\begin{aligned}\text{we have} \quad FT(\psi_{j,k}) &= 2^{\frac{j}{2}} FT(\psi(2^j t - kT_0)) \\ FT(\psi(2^j t)) &= \frac{1}{2^j}\Psi(\frac{\omega}{2^j}) \\ FT(\psi(2^j t - kT_0)) &= \frac{1}{2^j}e^{-i\frac{\omega}{2^j}kT_0}\Psi(\frac{\omega}{2^j}). \end{aligned} \quad (20)$$

Similarly for the scaling function, we have

$$FT(\phi(2^{J_0}t - kT_0)) = \frac{1}{2^{J_0}}e^{-i\frac{\omega}{2^{J_0}}kT_0}\Phi(\frac{\omega}{2^{J_0}}). \quad (21)$$

Hence

$$\begin{aligned}\gamma_{x_{\text{wavelet}}}(\omega) &= \frac{1}{T_0}\sum_{j=J_0}^{J-1}\sum_{k=0}^{2^j-1}2^{-j}|\Psi(\frac{\omega}{2^j})|^2 + \frac{1}{T_0}\sum_{q=0}^{2^{J_0}-1}2^{-J_0}|\Phi(\frac{\omega}{2^q})|^2 \\ &= \frac{1}{T_0}\sum_{j=J_0}^{J-1}|\Psi_j(\omega)|^2 + \frac{1}{T_0}|\Phi_{J_0}(\omega)|^2. \end{aligned} \quad (22)$$

Let us now consider the Haar wavelet, which is the oldest and simplest wavelet, and has a closed form expression in the time and frequency domain. The mother Haar wavelet and the mother Haar scaling function are expressed as follows

$$\psi(t) = \begin{cases} \frac{1}{\sqrt{T_0}} & \text{if} \quad 0 \le t \le \frac{T_0}{2} \\ -\frac{1}{\sqrt{T_0}} & \text{if} \quad \frac{T_0}{2} \le t \le T_0 \\ 0 & \text{else,} \end{cases} \quad (23)$$

$$\phi(t) = \begin{cases} \frac{1}{\sqrt{T_0}} & \text{if} \quad 0 \le t \le T_0 \\ 0 & \text{else.} \end{cases} \tag{24}$$

In order to express the PSD of Haar Wavelet-OFDM, let us first express $|\Psi(\omega)|$ and $|\Phi(\omega)|$.

$$\begin{aligned} \Psi(\omega) &= \int_{-\infty}^{+\infty} \psi(t) e^{-i\omega t} dt \\ &= i\sqrt{T_0} e^{-i\frac{\omega T_0}{2}} \frac{\sin^2 \frac{\omega T_0}{4}}{\frac{\omega T_0}{4}}, \\ |\Psi(\omega)| &= \sqrt{T_0} \left| \frac{\sin^2 \frac{\omega T_0}{4}}{\frac{\omega T_0}{4}} \right|. \end{aligned} \tag{25}$$

$$\begin{aligned} \text{Moreover} \quad \Phi(\omega) &= \frac{1}{\sqrt{T_0}} \int_{-\infty}^{+\infty} \phi(t) e^{-i\omega t} dt \\ &= \sqrt{T_0} e^{-i\omega T_0/2} \frac{\sin \omega T_0/2}{\omega T_0/2}, \\ |\Phi(\omega)| &= \sqrt{T_0} \left| \frac{\sin \omega T_0/2}{\omega T_0/2} \right|. \end{aligned} \tag{26}$$

From (22), (25), and (26), we obtain an expression for the PSD of Haar Wavelet-OFDM as follows

$$\gamma_{x_{\text{haar}}}(f) = \sum_{j=J_0}^{J-1} \left| \frac{\sin^2 \frac{\pi f T_0}{2^{j+1}}}{\frac{\pi f T_0}{2^{j+1}}} \right|^2 + |\text{sinc}(\pi f T_0/2^{J_0})|^2. \tag{27}$$

### B. Width of the main lobe

The width of the main lobe of the PSD gives a measure of the bandwidth efficiency of the signal. Here we calculate $\Delta f_{\text{haar}}$ of the PSD of Haar Wavelet-OFDM expressed in (27).

$$\begin{aligned} \gamma_{x_{\text{haar}}}(f) &= 0 \qquad (28) \\ &\Leftrightarrow \begin{cases} \forall j \in [J_0, J-1] & \left| \frac{\sin^2 \frac{\pi f T_0}{2^{j+1}}}{\frac{\pi f T_0}{2^{j+1}}} \right|^2 = 0 \\ \text{and} & |\text{sinc}(\pi f T_0/2^{J_0})|^2 = 0 \end{cases} \\ &\Leftrightarrow \begin{cases} \forall j \in [J_0, J-1] & \frac{f T_0}{2^{j+1}} = k_j, \quad k_j \in \mathbb{Z}^* \\ \text{and} & \frac{f T_0}{2^{J_0}} = k_L, \quad k_L \in \mathbb{Z}^* \end{cases} \\ &\Leftrightarrow \quad f T_0 = 2^J k, \quad k \in \mathbb{Z}^*. \qquad (29) \end{aligned}$$

The width of the main lobe is $\Delta f_{\text{haar}} = f_1 - f_{-1}$, such that $f_1 = \frac{2^J}{T_0}$ and $f_{-1} = \frac{-2^J}{T_0}$. We have then :

$$\Delta f_{\text{haar}} = \frac{2M}{T_0}. \tag{30}$$

Note here that the width of the main lobe is the same for all the variants, since it does not depend on the first scale $J_0$.

## IV. Simulations and Discussion

In this section, the PSD is obtained by simulation, to confirm the analysis in Section III, and the bandwidth efficiency of Wavelet-OFDM is discussed and compared with conventional OFDM.

### A. Simulation of the PSD of Haar Wavelet-OFDM

Fig.3 gives the experimental PSD, and the theoretical PSD as a function of the normalized frequency based on (27). The experimental PSD is simulated using Matlab, and estimated via the periodogram method with a rectangular window. Before applying the wavelet modulation based on IDWT, zero padding by a factor of 4 is performed on the input signal in the frequency domain. The number of carriers considered is $M = 16$. The experimental curve shows a good fit with the theoretical one.

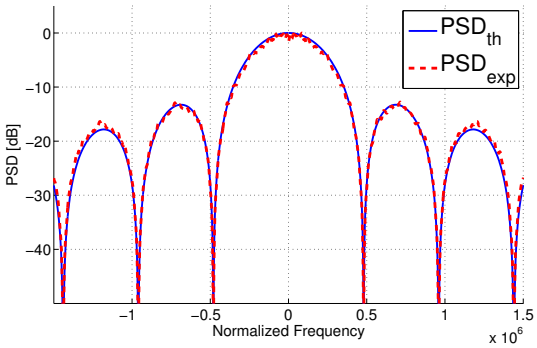


Figure 3: Theoretical and experimental PSD of Haar Wavelet-OFDM.

### B. Comparison with OFDM

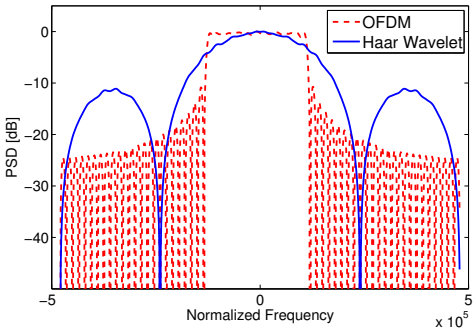


Figure 4: PSD of OFDM and Haar Wavelet-OFDM.

Based on the same parameters and method explained in Section IV-A, the PSD of Haar Wavelet-OFDM and OFDM without cyclic prefix are simulated as displayed in Fig.4. The width of the main lobe of the PSD of Haar Wavelet-OFDM is the double that of OFDM. Moreover, Haar Wavelet-OFDM has very large side lobes. Many applications can not tolerate these poor spectrum characteristics. It is true that Haar can be filtered to reduce the side lobes effect, but this will change the system performance. Note that OFDM may use a cyclic prefix, but it does not normally exceed 25% of the total bandwidth.

### C. Discussion

Fig.5 displays the sum over each scale of the wavelet in the frequency domain, and the sum over all the scales which gives the PSD as expressed in (19). As we can observe, the wavelets of the smallest scale have the largest main lobe width, and this defines the main lobe width of the PSD.

Among the well known wavelets, the Shannon wavelet has the best FL, but it is not orthogonal and has a slow decay in the time domain. In addition, the study investigates the DWT,

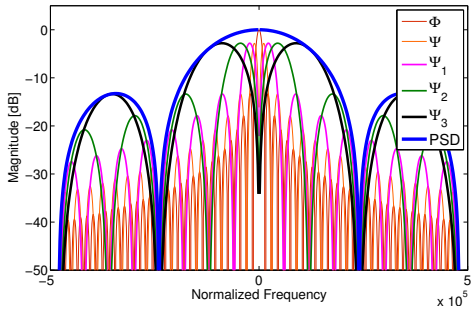


Figure 5: Frequency domain wavelets for each scale.

while the Shannon wavelet can be applied only to the complex wavelet transform. The Meyer wavelet is more attractive, as it has a faster decay and satisfies the orthogonality condition. A discrete format approximation of Meyer wavelet noted *Dmey* is possible, and it can simulate the Meyer wavelet based on a finite impulse response (FIR) filter as depicted in Fig.6 [1]. As a result, the fast wavelet transform can approximate the Meyer wavelet transform, and the DWT can be applied. As simulated

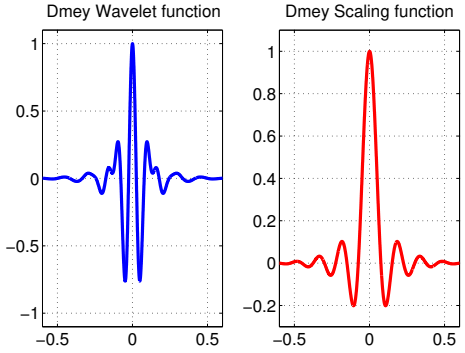


Figure 6: Discrete Meyer wavelet and scaling function.

in Fig.7, Discrete Meyer Wavelet-OFDM has a better spectrum efficiency than Haar Wavelet-OFDM, but it is not as good as OFDM without cyclic prefix.

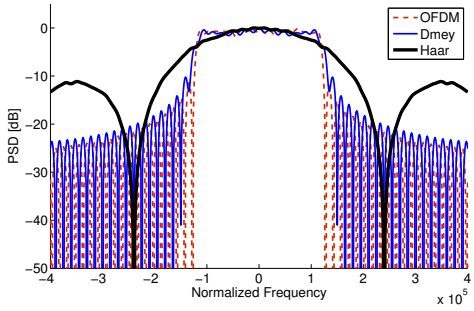


Figure 7: PSD of OFDM and Meyer Wavelet-OFDM.

[1]Generated using the MATLAB wavefun('dmey') command, Wavelet Toolbox.

## V. Conclusion

The PSD limitations of Wavelet-OFDM have been investigated in this paper, especially for the Haar wavelet. While Haar Wavelet-OFDM has some advantages, we have shown that it has a serious limitation in terms of the bandwidth efficiency, since its spectrum has large main lobe and large side lobes compared with the OFDM system.

Even though the Meyer wavelet is not as extensively promoted in the literature as the Haar wavelet, but has a better bandwidth efficiency, and may potentially compete with OFDM in this respect. Our next study is about the characteristics and performance of Meyer Wavelet-OFDM.

## Acknowledgements

This work has received a French state support granted to the CominLabs excellence laboratory and managed by the National Research Agency in the "Investing for the Future" program under reference Nb. ANR-10-LABX-07-01. The authors would also like to thank the Region Bretagne, France, for its support of this work.

## References

[1] Madan Kumar Lakshmanan and Homayoun Nikookar. A review of wavelets for digital wireless communication. *Wireless Personal Communications*, 37(3-4):387–420, 2006.

[2] Scott L Linfoot, Mohammad K Ibrahim, and Marwan M Al-Akaidi. Orthogonal Wavelet Division Multiplex: An Alternative to OFDM. *Consumer Electronics, IEEE Transactions on*, 53(2):278–284, 2007.

[3] Youbing Zhang and Shijie Cheng. A Novel Multicarrier Signal Transmission System over Multipath Channel of Low-voltage Power Line. *Power Delivery, IEEE Transactions on*, 19(4):1668–1672, 2004.

[4] Deepak Gupta, Vipin B Vats, and Kamal K Garg. Performance Analysis of DFT-OFDM, DCT-OFDM, and DWT-OFDM Systems in AWGN Channel. In *Wireless and Mobile Communications, 2008. ICWMC'08. The Fourth International Conference on*, pages 214–216. IEEE, 2008.

[5] Jamaluddin Zakaria and Mohd Fadzli Mohd Salleh. Wavelet-based OFDM Analysis: BER Performance and PAPR Profile for Various Wavelets. In *Industrial Electronics and Applications (ISIEA), 2012 IEEE Symposium on*, pages 29–33. IEEE, 2012.

[6] Waleed Saad, N El-Fishawy, S El-Rabaie, and Mona Shokair. An Efficient Technique for OFDM Dystem using Discrete Wavelet Transform. In *Advances in Grid and Pervasive Computing*, pages 533–541. Springer, 2010.

[7] Marius Oltean and Miranda Naforniţă. Efficient Pulse Shaping and Robust Data Transmission Using Wavelets. In *Intelligent Signal Processing, 2007. WISP 2007. IEEE International Symposium on*, pages 1–6. IEEE, 2007.

[8] Alaa Ghaith, Rima Hatoum, Hiba Mrad, and Ali Alaeddine. Performance Analysis of the Wavelet-OFDM New Scheme in AWGN Channel. In *Communications and Information Technology (ICCIT), 2013 Third International Conference on*, pages 225–229. IEEE, 2013.

[9] Swati Sharma and Sanjeev Kumar. BER Performance Evaluation of FFT-OFDM and DWT-OFDM. *International Journal of Network and Mobile Technologies*, 2(2):110–116, 2011.

[10] Kavita Trivedi, Anshu Khare, and Saurabh Dixit. BER Performance of OFDM with Discrete Wavelet Transform for Time Dispersive Channel. *International Journal of Research in Engineering and Technology*, 3:2319–1163, 2014.

[11] Stéphane Mallat. *A Wavelet Tour of Signal Processing*. Academic press, 1999.